Controlling dielectric film defects to increase the breakdown voltage of conductive polymer solid capacitors

David Quintero[1,*], *Hisato Matsuya*[2], *Mana Iwai*[1], *Sho Kitano*[1], *Koji Fushimi*[1], *Hiroki Habazaki*[1,*]

[1] Division of Applied Chemistry, Faculty of Engineering, Hokkaido University, Sapporo, Hokkaido 060-8628, Japan

[2] Graduate School of Chemical Sciences and Engineering, Hokkaido University, Sapporo, Hokkaido 060-8628, Japan

* e-mail: dalberto.quintero@eng.hokudai.ac.jp ; habazaki@eng.hokudai.ac.jp

Abstract

Aluminum solid polymer capacitors are promising devices for the increased demand for power electronics applications. Nonetheless, the low breakdown voltage of the commercially available (~100 V) limits their applications. In this study, a hydroxide film-covered high-purity aluminum was anodized at 700 V in boric acid at 85˚C, and the effect of second hot

water immersion (post-hydration treatment) after anodizing on the breakdown voltage was studied as a possible future treatment to enhance the withstand voltages of solid electrolytic capacitors. The dielectric breakdown voltage of the anodized aluminum with a PEDOT:PSS coating was ~500 V, being ~200 V less than the anodizing voltage; however, the dielectric breakdown voltage was increased above 700 V by introducing the post-hydration treatment due to the formation of a nanovoids layer above the dielectric alumina film. Our research suggests that the highly dispersed nanovoids incorporated with PEDOT:PSS avoid the current concentration at some local regions, effectively increasing the dielectric breakdown voltage. The post-hydration treatment increased the leakage current by introducing physical defects in the dielectric film. However, the leakage current was reduced by a voltage sweep below the breakdown voltage after the PEDOT:PSS coating or a second anodizing process before the coating, keeping the breakdown voltage above 600 V. A promising processing route to obtain aluminum solid capacitors with high withstand voltage (600 V) found in our research is first, dipping in hot water, second, anodizing at 700 V, then, a second hot water treatment, and a second anodizing at 400 V, which keeps the capacitance invariable with a breakdown voltage enhanced.

Keywords: solid aluminum capacitor, hot water treatment, PEDOT:PSS, anodizing, boric acid, breakdown potential.

1. Introduction

Aluminum electrolytic capacitors are used in many fields of electronics due to their excellent combination of dielectric properties, such as high capacitance, high withstand voltage, high energy density, and inexpensive cost.[1–3] Unfortunately, the disadvantages of these capacitors are related to the cathode given that the lifetime is limited mainly for the electrolyte evaporation and the high equivalent series resistance (ESR) that leads to overheating, a reduction in the ripple current and generates higher voltage fluctuations.[4,5] Several researchers have attempted to improve electrolytic capacitors to overcome those issues. Initially, the development of conductive organic salts was explored as a first solution for a solid electrolyte with better conductivity than liquid electrolytes (like TCNQ-7,7,8,8-tetracyanoquinodimethane or N-n-butyl isoquinolinium and TTF-tetrathiafulvalene)[6]. Then, aluminum solid polymer capacitors, which use a conductive polymer as a cathode, were developed in the 1990s as an alternative to aluminum electrolytic capacitors.[7] The first generation of polymer electrolytic capacitors was based on polypyrrole (PPy), followed by a second generation based on PEDOT [8–10], which has received a lot of interest due to its remarkable environmental stability [11,12]. PEDOT:PSS is more conductive, has better temperature stability than PPy or TCNQ, and can withstand short-term exposure to 280°C [13]. Furthermore, PEDOT:SS is not a toxic chemical (PPy is a toxic chemical), and when used in polymer capacitors, lower leakage currents are obtained than PPy. The high-temperature stability of PEDOT:PSS was the driving force behind its replacement with the less stable PPy polymer [14–16]. Therefore, the high thermal stability[17] and lower ESR increase the ripple current and capacitor's lifetime.[18–20] A disadvantage of aluminum solid electrolytic capacitors commercially available is the low breakdown voltages, limiting the operating voltage of the

commercially available capacitors to ~100 V or less, a lower value compared to ~500 V withstand voltage reached by electrolytic capacitors. Therefore, innovative capacitors with high thermal stability, high withstand voltages (~ 600 V), high capacitance, and high ripple current need to be developed for the next generation of power electronics systems, where aluminum solid polymer electrolytic capacitors show potential.[21–23] Although aluminum solid conductive polymer capacitors are commercially available, the scientific background is scarce, and the reasons for their low dielectric breakdown voltages are still unclear in the literature. Therefore, understanding the scientific phenomena will help implement strategies to improve their withstand voltage.

One possible hypothesis suggests that the properties and characteristics of the dielectric material likely influence the breakdown voltage.[24] The dielectric material used in aluminum capacitors is obtained by conventional anodizing, which is well known for forming amorphous oxide layers.[25–27] Nevertheless, in anodizing aluminum, a barrier-type alumina oxide layer, either amorphous or crystalline, can be obtained, depending on the growth conditions. Simple hot water treatment of the aluminum before anodizing allows the formation of a hydrous oxide (with a structure like pseudo-boehmite $Al_2O_3 \cdot xH_2O$),[28–30] which then during anodizing in neutral borate solution at high temperature works as crystallization seeds that induce the formation of a crystalline alumina layer with a structure like ɣ'-Al_2O_3 (a defect spinel structure like ɣ-Al_2O_3 but with more disorder in the cation lattice).[31,32] The lower ionic conductivity of the crystalline alumina and the higher dielectric constant provide higher capacitance and higher breakdown voltage with a thinner dielectric layer compared to the amorphous oxide. Therefore, the crystalline oxide layers are preferable due to their dielectric properties, especially for medium and high-voltage capacitors.[33–35] The

amorphous-to-crystalline transformation results in a denser oxide followed by shrinkage, which leaves microscopic voids, cracks, and high-stress levels [36]. The introduction of such physical defects often increases the leakage current or reduces the withstand voltage of the capacitor. So, the industrial manufacturing of dielectric layers by anodizing on aluminum involves multi-steps,[37,38] including multiple re-anodizing processes that can reduce the leakage current caused by the defects formed during the crystallization.[39] Sato et al.[40] studied the effect of electrolyte species and their combination during multi-steps of anodizing of hydroxide film-covered aluminum, showing that re-anodizing, especially in borate electrolyte, effectively reduces the leakage current. On the other hand, in aluminum electrolytic capacitors, leakage current is increased after a storage time due to the dielectric defects caused by chemical reactions in the capacitor when there is no applied voltage. When a voltage is applied, the electrolyte can impregnate and heal such physical defects, contributing to dropping the leakage current, which reflects the repair phenomenon of the dielectric layer defects.[41,42] It has been suggested that an electrolyte-free conductive polymer cannot be impregnated adequately in a porous dielectric material, limiting the repair of the dielectric defects.[19] Nonetheless, the little literature evidence on anodic oxide layers obtained at high voltages and coated with a conductive polymer does not allow conclusions about the phenomena in solid polymer capacitors at high voltages [7].

This research focused on assessing the performance of aluminum solid polymer conductive capacitors at high voltages. Our research proposes a new treatment to increase the breakdown potential of the aluminum solid polymer capacitor, which consists of a hot water immersion of the anodic layer after anodizing, in addition, the healing of the dielectric defects in an electrolyte-free conductive polymer capacitor was studied by voltage sweep below

breakdown and second anodizing process. A commercial poly (3,4-ethylene dioxythiophene): poly(4-styrene sulfonic acid) (PEDOT:PSS) conductive polymer was used to make the aluminum solid polymer capacitor, which has low ESR and high thermal stability [3,43]. A hydroxide film-covered high-purity aluminum was anodized at 700 V in boric acid at 85˚C, with subsequent post-hydration treatment. With the post-hydration after anodizing, the breakdown voltage was above 700 V, which is ~200 V higher than the breakdown voltage after anodizing ~514 V. Nonetheless, the leakage current was increased after the post-hydration treatment due to the formation of nanovoids generated after the post-hydration treatment and its connection with the voids in the dielectric layer near the metal/oxide interface. Contrary to the general view that the defects in the dielectric film should be breakdown sites, the above results indicate that the breakdown voltage was enhanced after the number of voids on the dielectric layer was increased in a controlled way. In addition, the high leakage current was reduced by two methods: a voltage sweep below the dielectric breakdown voltage after the PEDOT:PSS coating and a re-anodizing before the coating.

2. Experimental

2.1. Dielectric material formation. A 99.99 % pure aluminum sheet with a 15 × 80 × 0.5 mm dimension was used for the dielectric material formation. The aluminum sheet was electropolished in a 60% $HClO_4$/ethanol solution at 20 V for 5 min at a temperature lower than 10˚C. To guarantee a crystalline oxide formation, a hydrous oxide layer was formed by dipping the electropolished aluminum in hot Milli-Q water at 95°C for 10 min. The pretreated aluminum sheet was anodized at a constant voltage of 700 V, applying an initial current density of 10 mA cm^{-2} in a 0.5 mol L^{-1} boric acid solution at 85°C for 10 min. A 0.5 L two-

electrode cell with an aluminum foil as a counter electrode was used for anodizing. Once anodizing was finished, samples were washed with Milli-Q water and dried with a cool air stream.

2.2. Post-anodizing treatments. Additional treatments were performed on the anodized aluminum, as described below. A second boiling water treatment was done by dipping the anodized aluminum in hot Milli-Q water at 95°C for 10 min (post-hydration treatment). The second anodizing process was done by re-anodizing the anodized aluminum with post-hydration treatment by applying a constant voltage in a 0.5 mol L^{-1} boric acid solution at 85°C for 10 min. The re-anodizing voltages evaluated were 200, 400, and 630 V.

2.3. Aluminum solid polymer configuration. A conductive polymer solid capacitor was made using the anodic layer obtained by anodizing as a dielectric material and a solid coating of PEDOT:PSS (a conductive polymer) as a cathode. The polymer coating was obtained by dropping a PEDOT:PSS dispersion solution with a pH 3-4 (1wt% of PEDOT:PSS commercial Agfa dispersion containing 0.0018 mol L^{-1} ethylene glycol and 0.00028 mol L^{-1} sorbitol) in an area of 10 mm in diameter and dried at 110°C, with an outer graphite/silver connection. The PEDOT:PSS dispersion viscosity is ~8 mPa s and was evaluated using a viscometer (A&D, SV-10a). Four sites were evaluated in the anodized hydroxide film-covered aluminum with dimensions of 10 mm in diameter. The details of the capacitor configuration are shown in the supporting information, Fig. S1.

2.4. Surface and cross-section observations. The surface and cross-section samples were observed by a field-emission scanning electron microscope (ZEISS, Sigma-500), operated at 1 kV. The SEM cross-section samples were produced by a broad ion milling technique (JEOL, IB-19530CP). The Al/ɣ'- Al_2O_3/PEDOT:PSS cross-sections were assessed using a scanning transmission electron microscope (JEOL, JEM-ARM200F), operated at 200 kV and equipped with EDS facilities. A focused ion beam system (JEOL, JIB4601F) was used to create electron-transparent sections. Elemental depth profiles of the Al/ɣ'- Al_2O_3/PEDOT:PSS were obtained by a glow discharge optical emission spectrometer (GDOES: Horiba-Jobin Yvon, 5000 RF).

2.5. Capacitor electrical properties. AC impedance spectra were obtained using a potentiostat/galvanostat (Biologic, SP-200) equipped with a frequency response analyzer, applying an amplitude of 50 mV AC in a frequency range from 7 MHz to 0.1 Hz. A two-electrode cell configuration was used, and two different capacitor configurations were evaluated. One capacitor configuration comprises Al/ɣ'- Al_2O_3/PEDOT:PSS, with the Al/ɣ'- Al_2O_3 as an anode and the PEDOT:PSS solid coating as a cathode. Another capacitor configuration comprises Al/ɣ'- Al_2O_3/0.1 mol L^{-1} ammonium pentaborate, with the Al/ɣ'- Al_2O_3 as an anode and the ammonium pentaborate solution as a cathode (See Fig. S2). An area of 10 mm in diameter was assessed by AC impedance, which was demarcated using a PTFE Film-based adhesive tape (Nitto Denko, P-422 NAT).

The leakage current and breakdown voltage of the solid capacitors were assessed by current-voltage curves obtained by voltage sweeping at a rate of 1 V s^{-1} using a source measure unit (Keithley, 2410).

3. Results and Discussion

3.1. Dielectric layer formation and the effect of post-hydration treatment. Figure 1 shows surface (SEM analysis) and cross-section (STEM analysis) images for the anodized samples. The surface images were observed before the PEDOT:PSS coating and the cross-sections were imaged after the coating. The hot water reaction offers the ability to grow metal oxide nanostructures[28,44] due to forming a lamellae structure oriented approximately perpendicular to the substrate surface, which consists of pseudo-boehmite, as it is well known in the literature.[45,46] The pseudo-boehmite structure obtained remains after anodizing and the second boiling water treatment, and no differences are observed from the surface observations (Fig. 1a and 1d). From the cross-section images (Fig. 1b and 1c) of the dielectric layer after anodizing, a dual layer structure is observed with an inner oxide layer with a thickness of ~680 nm and an outer porous lamellae pseudo-boehmite layer with a thickness of ~140 nm. Some micro-voids are observed near the metal/oxide interface (black regions pointed with arrows in Fig. 1b), while the outer region of the oxide layer shows a dense structure. The dielectric layer shows a crystalline structure with an arrangement like ɣ'- Al_2O_3 according to the SAED patterns (interplanar spacing was compared to the reference ICSD 98-003-0267),[47] being consistent with the previous studies of anodizing hydroxide film-covered aluminum in neutral solutions.[31,48–51] Voids are the result of the crystallization, which results in volume shrinkage of the oxide during anodizing; in addition, the conversion leads to an inward movement of crystalline/amorphous interface accompanied by void transport, increasing voids volume and position through the oxide layer, which explains the voids generated in the dielectric layer (Fig. 1b and 1e; pointed with arrows).[24,52] The post-hydration treatment (Fig. 1e-1f) thickens the outer porous lamellae layer, increasing the

thickness to ~270 nm while the oxide layer thickness remains unchanged. Furthermore, the formation of nanovoids in the hydrated layer/oxide interface is evidenced, showing a highly dispersed and homogenous distribution with a depth penetration of ~150 nm (Fig. 1e). The post-hydration treatment does not change the crystalline structure obtained after anodizing even in the region where the nanovoids were generated (Fig. 1f).

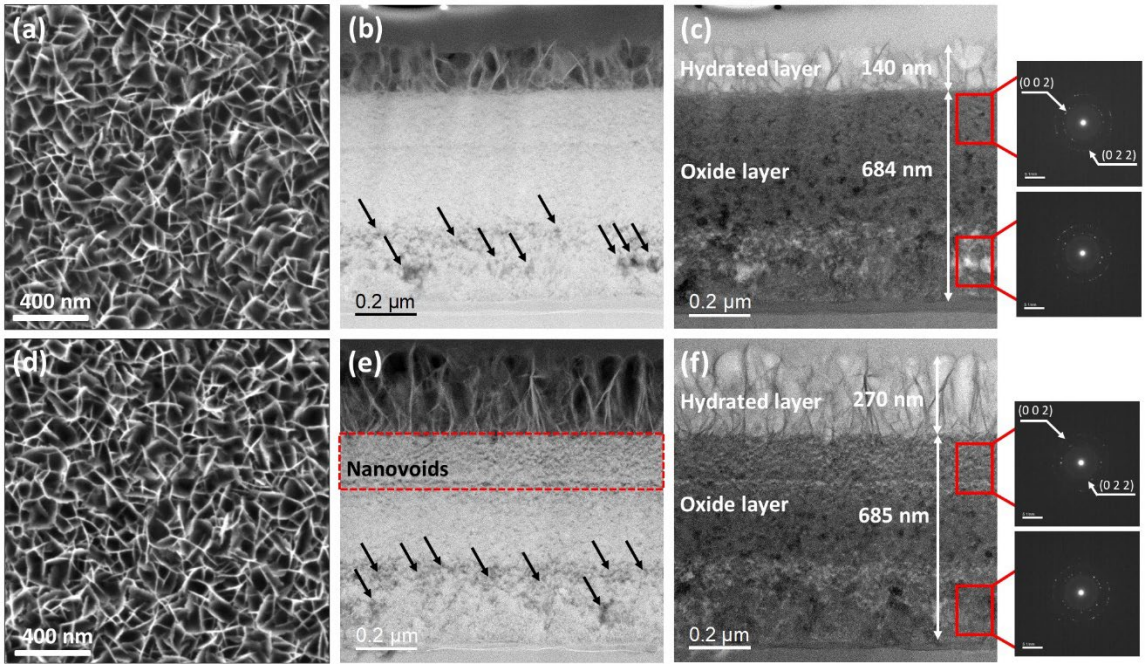

Figure 1. Surface SEM images of the outer hydrated layer obtained by anodizing at 700 V (a) before and (d) after the post-hydration treatment. (b, e) HAADF and (c, f) BF scanning transmission electron micrographs of the cross-sections for the anodized aluminum covered with PEDOT:PSS polymer; (b, c) without and (e, f) with post-hydration treatment. SAED patterns were included in (c, f).

The elemental distribution assessed by GDOES of the anodized aluminum covered with PEDOT:PSS polymer is observed in Fig. S3. Sulfur and carbon profiles suggest that the polymer penetrates the porous hydrated layer. At the same time, boron is incorporated from the anodizing electrolyte species into the outer region of the oxide layer, as boron is known to be incorporated in the oxide layer during anodizing.[53] The voids shown in Fig. 1b are mainly generated in the boron-free inner region of the barrier layer because less crystalline alumina is developed in the boron-containing region.[33] The EDS analysis (Fig. 2) evidenced a homogeneous distribution of Al and O due to the oxide layer obtained; the dark regions in the oxide layer correspond to the voids obtained during the anodizing process, which fit with dark regions in the EDS elemental mapping. The S signal helps to elucidate the interaction of the PEDOT:PSS polymer in both the hydrated and the alumina layers, where it is evidenced that the porous pseudo-boehmite contains PEDOT:PSS. An EDS area analysis reveals the interaction of the PEDOT:PSS with the dielectric layer (Fig. 3). After anodizing, PEDOT:PSS polymer covers the porous hydrated layer and penetrates up the hydrated/oxide interface as it is evidenced in Fig. 3a. The post-hydration treatment induces the formation of a nanovoids layer, which the PEDOT:PSS dispersion can penetrate, as it is observed in the EDS area analysis (Fig. 3b). An in-detail analysis shows that the polymer penetrates approximately ~150 nm from the hydrated layer/oxide interface which results in a decrease in the dielectric layer thickness (Fig. 3c). It is concluded that after anodizing, the dielectric layer thickness is controlled by the oxide layer thickness (~684 nm), but after the post-hydration treatment, the dielectric layer is controlled by the thickness of the PEDOT:PSS free Al_2O_3 layer (~535 nm).

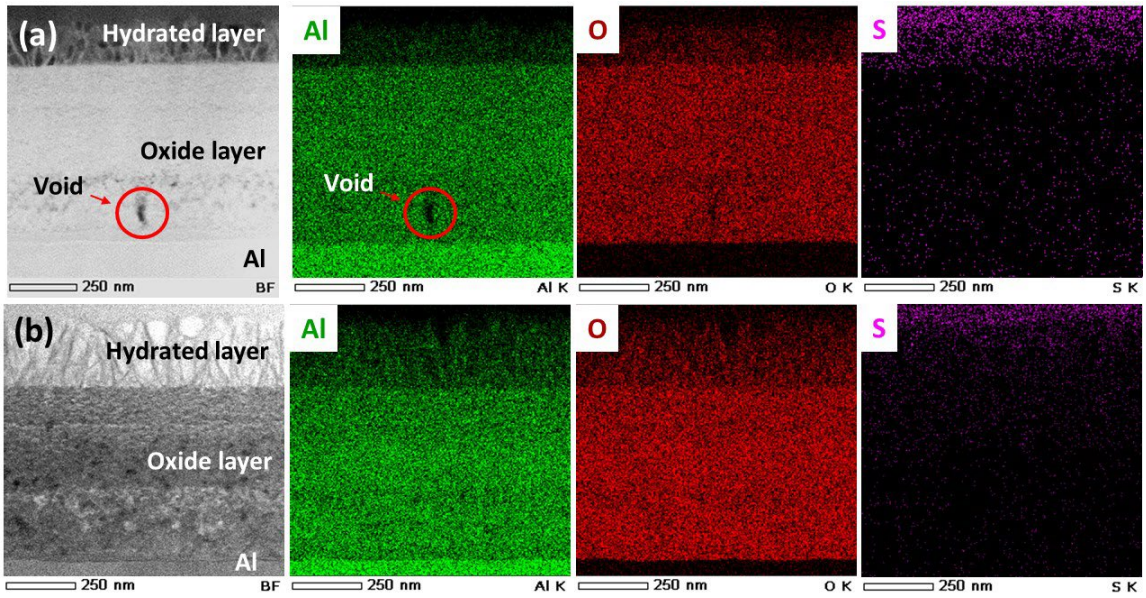

Figure 2. EDS elemental mapping of the cross-sections of the anodized aluminum covered with PEDOT:PSS polymer after (a) anodizing at 700 V and (b) anodized with post-hydration treatment.

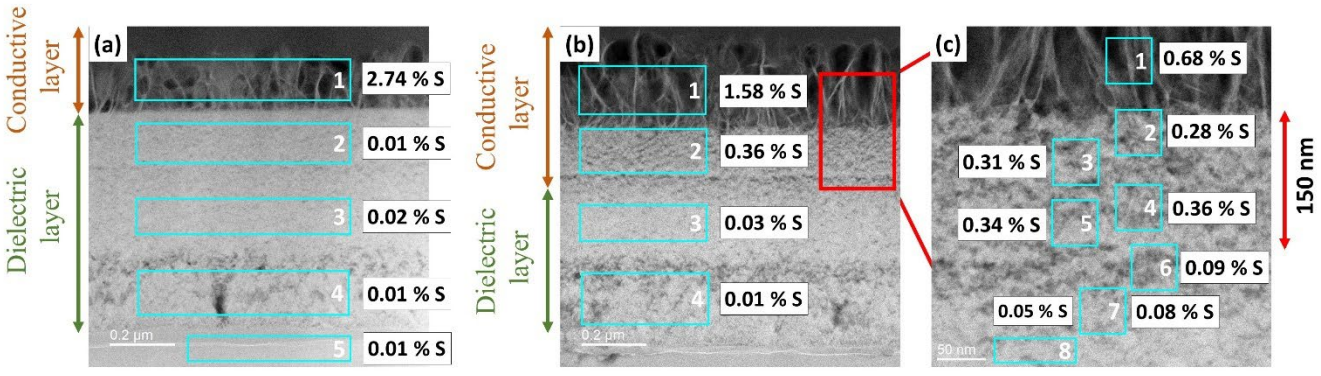

Figure 3. EDS area analysis of the anodized aluminum cross-sections covered with PEDOT:PSS polymer: (a) after anodizing and (b, c) after the post-hydration treatment. EDS spectra and elemental composition are reported in the supporting information (Fig. S6-S8; Table S1-S3).

The electrical properties of the capacitors were assessed by AC impedance spectroscopy. Two capacitor configurations were assessed: the aluminum solid polymer capacitor with the PEDOT:PSS as a cathode and the aluminum electrolytic capacitor with an aqueous solution of 0.1 mol L^{-1} ammonium pentaborate solution as a cathode. For the dielectric layer after anodizing (Fig. 4a), impedance decreases linearly with the frequency in the double logarithmic plot with similar behavior for both cathodes up to 100 kHz, and then the resonant frequency behavior changes in both cathodes due to differences in the ESR (Table 1). The low ESR in the PEDOT:PSS generates a lower impedance at higher frequencies than the aqueous electrolyte cathode [42]. The ideal behavior of a dielectric material shows a phase shift near 90˚, which is evident below 1 MHz and 10 kHz for the capacitor with PEDOT:PSS and the capacitor with the aqueous electrolyte cathode, respectively. Capacitance and ESR were assessed by fitting the experimental results with the equivalent circuit shown in Fig. 4c [42,54]. The capacitance value in liquid electrolyte and PEDOT:PSS polymer present close values (~10% difference), which is related to the fact that both liquid electrolyte and solid polymer penetrated the porous pseudo-boehmite layer. The slight variation is based on the viscosity difference (~8 mPa s for PEDOT:PSS dispersion and 1.06 mPa s for the liquid electrolyte). Using the equation of a parallel plate capacitor,[4] with a dielectric layer thickness of 684 nm, an area of 0.785 cm^2 and a capacitance of 10.4 nF cm^{-2} in the PEDOT:PSS configuration, the dielectric constant of the dielectric layer is 10.2 (Table 3), corresponding to the dielectric constant for ɣ'-Al_2O_3.[55–57] After post-hydration treatment (Fig. 4b), the impedance shows a linear tendency with frequency like the as-anodized condition; nonetheless, the slope changes for both capacitors. At frequencies higher than 100 kHz, the resonant frequency is clearly defined only for PEDOT:PSS capacitor due to the low ESR. A deviation from the ideal

dielectric behavior is observed from the phase shift vs. frequency plot, where a phase shift lower of 90˚ at lower frequencies is observed for the solid capacitor with PEDOT:PSS. The frequency range analysis was done from 100 Hz to 7 MHz for the experimental results analysis by the equivalent circuit due to the deviation of the ideal capacitor behavior at low frequencies after the post-hydration treatment. The solid aluminum capacitor with PEDOT:PSS and post-hydration treatment shows a capacitance around 22 % higher than the solid aluminum capacitor after anodizing (as-anodized condition) due to the decrease in the dielectric layer thickness caused by the PEDOT:PSS penetration into the nanovoids layer (See Fig. 3c). On the other hand, in the liquid electrolyte, the AC impedance spectrum deviates largely from the ideal one of a capacitor so that the spectrum could not fit well using the equivalent circuit shown in Fig. 4c. Thus, the reliable capacitance value was not obtained. The large deviation from the ideal spectrum suggests the electrolyte penetration into the voids in the dielectric alumina layer as a consequence of the possible transformation of the closed voids to the open voids in the alumina layer by the post-hydration treatment.

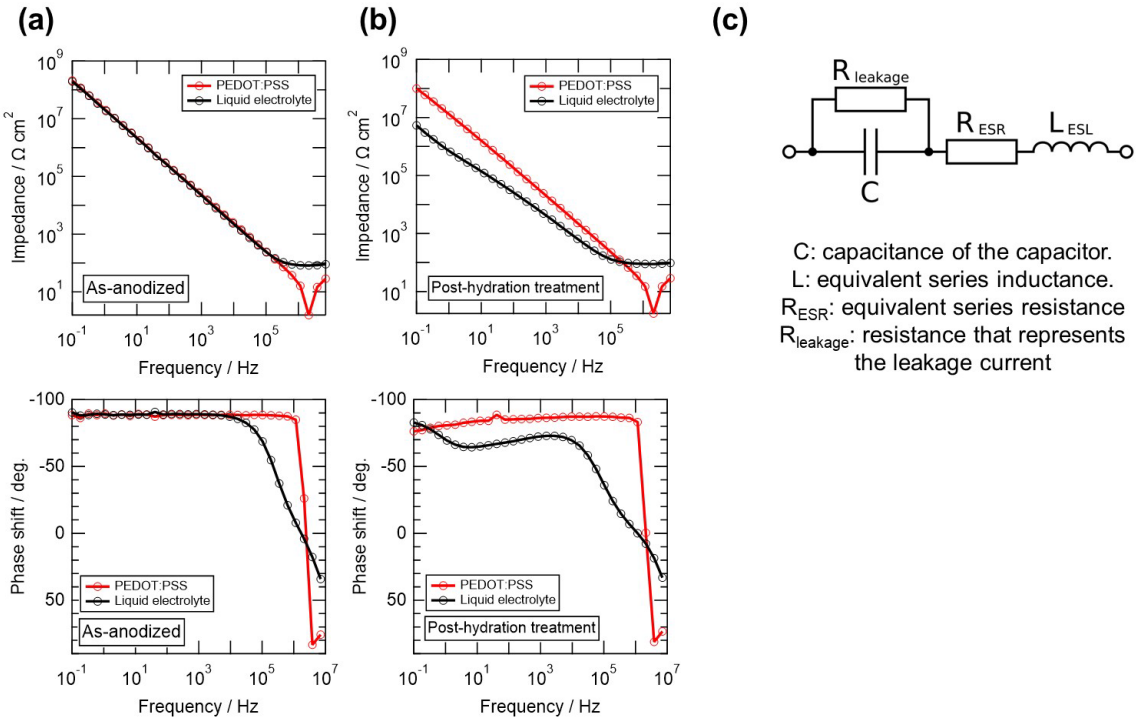

Figure 4. Bode plots of the aluminum (a) as-anodized, (b) anodized with a post-hydration treatment, and (c) the equivalent circuit used for fitting.

Table 1. Capacitance and resistance of the anodized aluminum and the subsequent post-hydration treatment after anodizing.

Cathode	Condition	Capacitance, C ($nF\ cm^{-2}$)	R_{ESR} ($\Omega\ cm^2$)
PEDOT:PSS	As anodized	10.44 ± 0.08	0.89 ± 0.06
	Post-hydration treatment	12.79 ± 0.30	1.40 ± 0.04
Aqueous electrolyte	As anodized	11.57 ± 0.22	52.06 ± 1.45
	Post-hydration treatment	-	-

The breakdown voltage of the capacitors was evaluated by a voltage sweep at 1 V s^{-1} to reach dielectric breakdown, which is identified by the sudden increase of the current up to 10 mA cm^{-2} and the sparking phenomenon in the capacitor (Fig. 5). From the current-voltage plots, the breakdown voltage and the leakage current behavior are observed in the solid conductive polymer capacitors. For the dielectric layer after anodizing (Fig. 5a), a low leakage current is evidenced during the voltage sweep below the breakdown voltage. The average breakdown voltage is 514 V, being ~200 V less than the anodizing voltage (700 V). The anodizing process of hydroxide film-covered aluminum involves the formation of voids and defects in the dielectric layer due to the nature of the amorphous-to-crystalline transformation at high anodizing voltages,[34] so, the higher the anodizing voltage, the higher the density of voids and defects in the dielectric layer, which increases the gap between the anodizing voltage and the breakdown voltage.[33] After the post-hydration treatment, the breakdown voltage increased markedly with an average value of ~790 V, above the value of the anodizing voltage (Fig. 5b). Nonetheless, a high leakage current is observed from low voltages, being related to nanovoids generated after the post-hydration treatment and its connection with the voids in the dielectric layer near the metal/oxide interface. The fundamental aspect of the post-hydration treatment is the homogeneous distribution (Fig. 1e) of the nanovoids generated in the outer region of the oxide layer, which distributes the current uniformly, contrary to a situation observed after the anodizing, where defects and voids are randomly distributed (Fig. 1b). Increasing the number of nanovoids to increase the breakdown voltage contrasts with the general opinion in the literature, where voids and defects are generally considered to be dielectric breakdown sites. Table 2 compares the results obtained in this study with literature reports on aluminum capacitors. In aluminum

solid polymer capacitors, at low anodizing voltages (up to 100 V), the breakdown voltage is close to or equal to the anodizing voltage; nevertheless, at high anodizing voltages (up to 1000 V), the gap between the breakdown voltage and the anodizing voltage is remarkable-as was evidenced in this research- and the reason for the low breakdown potential is unclear in the literature. Our research reports a breakdown voltage higher than the anodizing potential by performing a post-hydration treatment of the dielectric layer, a phenomenon that is not observed even in aluminum electrolytic capacitors [44,58,59]. On the other hand, in high-voltage aluminum electrolytic capacitors, etched aluminum foils with many tunnel pits have been used to reach a high capacitance due to the high surface area.[37,60,61] For increasing the breakdown voltage, a thicker dielectric layer is usually developed by applying higher anodizing voltages (~1000 V) [38], dramatically reducing the capacitance value due to the high dielectric layer thickness and the sealing of the tunnel pits. Consequently, the post-hydration treatment is a promising and simple treatment to enhance the breakdown voltage of solid conductive polymer capacitors and avoid a dramatic reduction in capacitance.

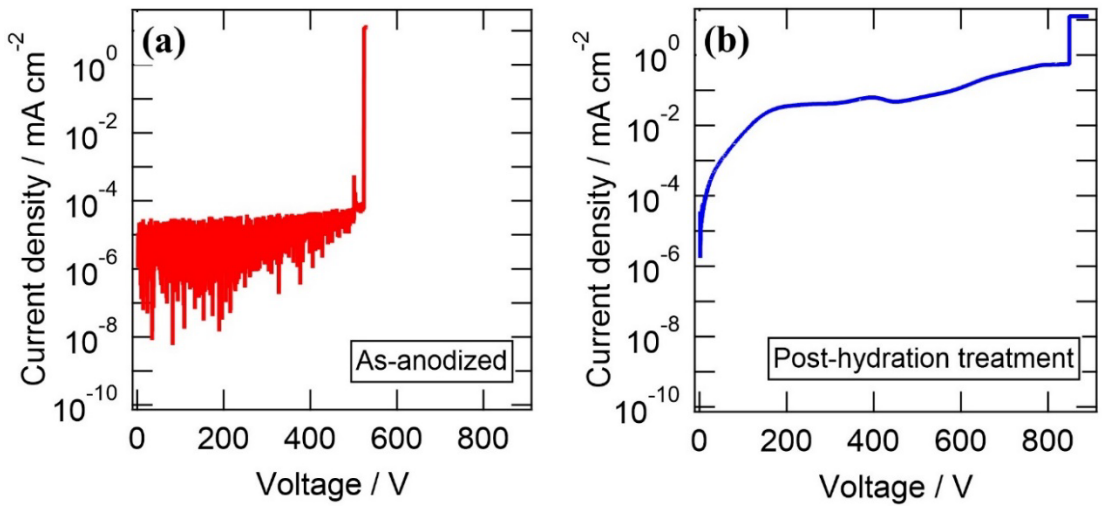

Figure 5. V-I responses of the anodized aluminum covered with PEDOT:PSS polymer obtained by (a) anodizing at 700 V (b) and anodized with post-hydration treatment. Measurement reproducibility is reported in the supporting information (Fig. S4).

Table 3 and Figure 6 summarize the results obtained in the aluminum anodized at 700 V and the subsequent post-hydration treatment. After post-hydration treatment, the formation of nanovoids generates a highly resistive interphase layer in the hydrated layer/oxide interface. The slight increase in the ESR value after the post-hydration treatment may suggest the high electrical resistivity of the thin nanovoids layer (Table 1). Therefore, the current concentration at some local defects that cause the dielectric breakdown is avoided. This fact was seen from the low-intensity sparking above the breakdown voltage for the sample with the post-hydration treatment. In contrast, local intense sparking was found for the sample without the nanovoid layer, as schematically illustrated in Fig. 6. The breakdown voltage increase after the post-hydration treatment is the most crucial consequence generated by a simple hot water treatment of the dielectric layer formed by anodizing, which is higher than

1 the anodizing voltage. The slight increase in the capacitance is associated with the
2 PEDOT:PSS penetration into the nanovoid layer formed at the upper part of the dielectric
3 layer, reducing the dielectric layer thickness. The formation ratio (nm V^{-1}) agrees with the
4 literature values for anodizing hydroxide film-covered aluminum.[33]
5
6 **Table 2.** Comparison between the results obtained in this research with literature reports

Anode	Cathode	Anodizing condition	Additional process	Dielectric layer thickness (nm)	Breakdown potential (V)	Reference
Al_2O_3	TNCQ salt	50 V Boric acid-borate solution	--	--	55 V	[62]
	TNCQ salt	200 V Boric acid-borate solution	--	--	176 V	[62]
	PEDOT:PSS	500 V 0.5 M H_3BO_3	--	470	~350 V	[35]
	PEDOT:PSS	700 V 0.5 M H_3BO_3		684	514 V	This study
	PEDOT:PSS	700 V 0.5 M H_3BO_3	Post-hydration treatment	535	790 V	This study

7
8 **Table 3.** Summary of the dielectric layer characteristics obtained after anodizing and the
9 subsequent post-hydration treatment for the aluminum solid conductive polymer capacitors.

Condition	Breakdown voltage (V)	ɣ'-Al_2O_3 coating thickness (nm)	Dielectric layer thickness (nm) [1]	Dielectric[2] constant ε_r	Formation ratio nm V^{-1}
As anodized	514 ± 24	684	684	10.2	0.98
Post-hydration treatment	790 ± 72	685	~ 535	9.86	--

10 [1]Dielectric layer thickness is related to the PEDOT:PSS-free region in the alumina (ɣ'-
11 Al_2O_3) layer.

12 [2] The dielectric constant was calculated from the equation of a parallel plate capacitor.

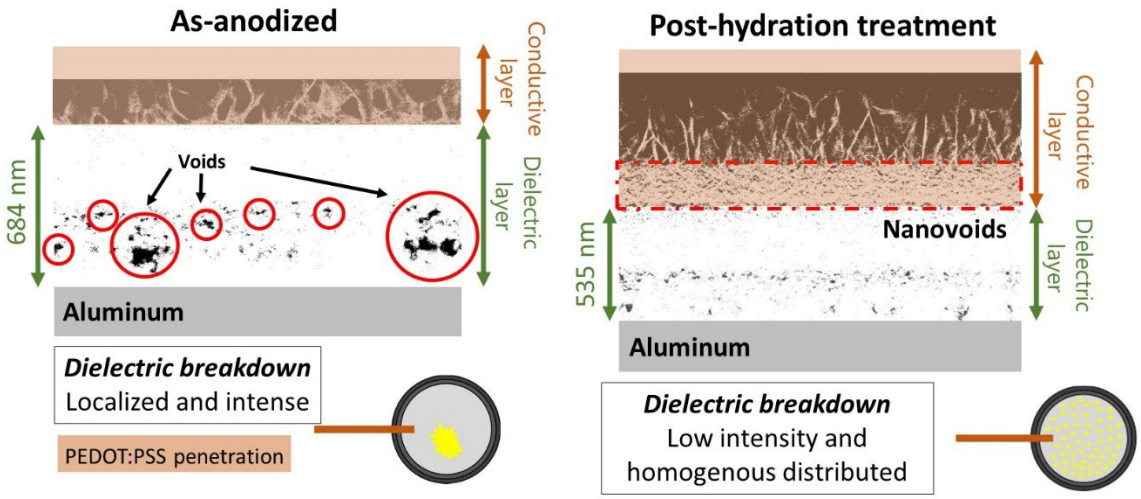

Figure 6. Graphical illustration of the effect of the post-hydration treatment on the dielectric layer defects and its effects on the dielectric breakdown.

3.2. Healing process of defects in the dielectric layer after post-hydration treatment.

As mentioned above, aluminum solid conductive polymer capacitors have many advantages over aluminum electrolytic capacitors. They stand out in high thermal stability, low ESR, high ripple current, and low voltage fluctuations; nonetheless, their low breakdown voltage of ~100 V limits their applications.[63,64] The current market demands capacitors with a maximum withstand voltage of up to 600 V, with a normal operating voltage range of up to 400 V.[65] Immersion of the dielectric layer in hot water after anodizing is a promising treatment to increase the breakdown voltage without reducing the capacitance. However, the high leakage current could lead to overheating of the capacitor, causing a decrease in the filtering performance, polymer degradation, and reducing the capacitor's lifetime. Different strategies have been found in the capacitor industry to reduce the leakage current by healing the defects in the dielectric layer. One approach during dielectric layer formation is to perform a multi-step anodizing to reduce the leakage current caused by the healing of the

dielectric defects formed by the crystallization.[34] In addition, in aluminum electrolytic capacitors, long-time storage increases the leakage current due to imperfections in the dielectric material caused by the chemical reactions inside the capacitor. Nonetheless, when a voltage is applied to the capacitor, the dielectric material can be regenerated by natural oxidation of the defects and leakage current density drops, reflecting a repair phenomenon of the dielectric layer [42]. In the metalized film capacitors, the self-healing of the dielectric has also been reported, preventing the risk of dielectric breakdown. The self-healing mechanism in metalized film capacitors differs from that of aluminum electrolytic capacitors, where the energy during discharging in the former is used to vaporize the metallization around the defect, thereby electrically isolating it [41]. Nevertheless, the scientific evidence of the healing process of the defects in the dielectric layer in aluminum solid polymer capacitors is scarce. In this study, two healing processes of the dielectric defects were evaluated, with the aim to reduce the high leakage current generated by the dielectric defects originated by the post-hydration treatment after anodizing. First, voltage sweeping from 0 to 400 V, a range below the breakdown voltage (~790 V), was evaluated in the solid conductive polymer capacitor with post-hydration treatment such as an in-situ "self-healing" process of the dielectric defects. Second, a re-anodizing process to repair the dielectric layer defects was evaluated on the anodized aluminum with post-hydration treatment. After the re-anodizing process was completed, the solid polymer capacitor was fabricated as described in the experimental section, and the breakdown voltage was evaluated by voltage sweeping at 1 V s^{-1} to reach the breakdown with sparking.

Figure 7a shows the current-voltage curves for the voltage sweep below the breakdown voltage. The first two voltage sweep cycles were conducted from 0 to 400 V, and the last

cycle was from 0 V to the breakdown voltage. From the first two voltage sweep cycles (Fig. 7a, black and red lines), the leakage current decreases, especially at low voltages, and the last voltage sweep cycle shows a reduced leakage current up to ~200 V. Then, the leakage current increases until it gets stable at ~500 V, showing a similar leakage current to the capacitor without healing the dielectric defects (Figure 5b). The breakdown voltage of the solid conductive polymer capacitor did not change by the voltage sweep cycles below the breakdown voltage. The current-voltage curves for the re-anodized aluminum are shown in Fig. 7b. The second anodizing process effectively reduces the leakage current; nonetheless, the breakdown voltage remains above 600 V only for the re-anodizing voltages of 200 and 400 V. When a voltage of 630 V is applied in the second anodizing process, a low leakage current is observed until the dielectric breakdown and a value below 600 V, close to the value obtained after the first anodizing process (~500 V). From the conditions evaluated in the second anodizing process, the second anodizing voltage of 400 V keeps the leakage current low from 0 to 400 V and the breakdown voltage above 600 V. The voltage sweep below the breakdown voltage and the second anodizing process heal the voids in the dielectric layer, and the decrease in current reflects the repair phenomenon of the dielectric defects. Nonetheless, different behavior is observed in both void healing processes, even when the same voltage is applied. Of the voltage sweep cycles and the second anodizing process at 400 V, the second anodizing process effectively reduces the leakage current up to 400 V since the liquid electrolyte can impregnate in an effective way the defects in the dielectric layer than PEDOT:PSS dispersion. The self-healing process in solid polymer capacitors at low voltages has already been reported;[7] nonetheless, our research found scientific evidence of the healing of dielectric defects in aluminum solid polymer capacitors at high voltages with

a new promising treatment to enhance the breakdown voltage, which is the post-hydration treatment after anodizing.

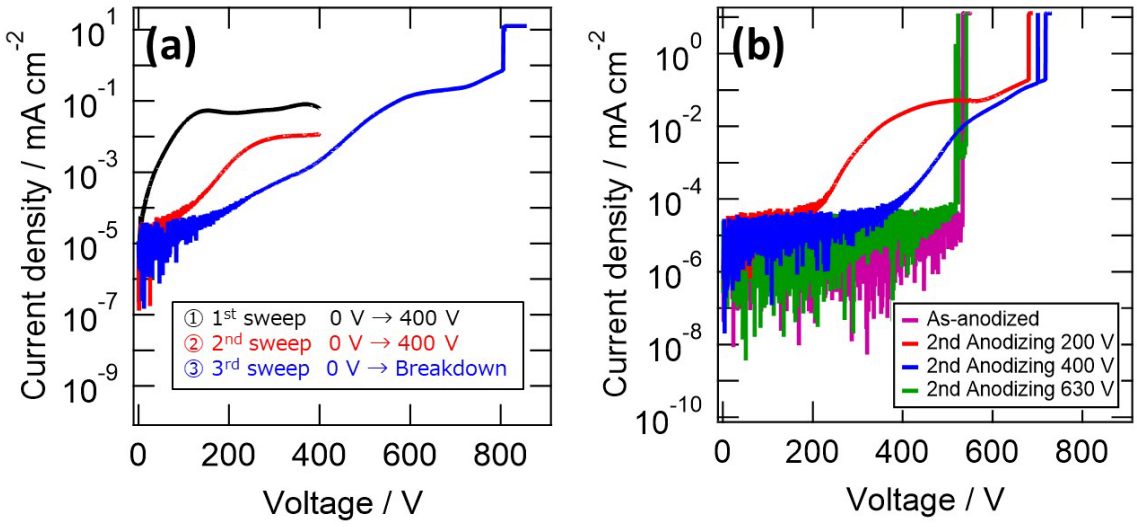

Figure 7. Current-voltage curves of anodized aluminum with a post-hydration treatment covered with PEDOT:PSS polymer after (a) the voltage sweep from 0 to 400 V, (b) the re-anodizing process at 200, 400, and 630 V voltages. Measurement reproducibility is reported in the supporting information (Fig. S5).

SEM surface and cross-section images of the dielectric layer after the second anodizing process are shown in Fig. 8. From surface SEM, no significant changes are observed in the surface morphology of the dielectric after the second anodizing at different anodizing voltages (Fig. 8a, 8c, 8e). SEM cross-section images evidence the healing of the dielectric defects by the second anodizing process. The healing of the dielectric defects starts from the metal/oxide interface, which is possible given that liquid electrolytes can impregnate the

defects and the voids in the dielectric layer through the oxide thickness, and the thickness of the repaired defects is related to the formation ratio, which is ~1 nm V^{-1}.[33,66,67]. For the second anodizing at 200 V, some voids above the thickness of ~200 nm from the metal/oxide interface are still present, in addition to the nanovoids obtained after the post-hydration treatment (Fig. 8b). The repair of the dielectric layer reduced the leakage current from 0 to 200 V, and then the leakage current is increased until the dielectric breakdown. A similar behavior is evidenced after the second anodizing process at 400 V; voids in the dielectric layer are healed, and the nanovoids formed with the post-hydration treatment are still present (Fig. 8d). The leakage current is low from 0 to 400 V and then is increased until the dielectric breakdown. In contrast, the second anodizing at 630 V shows a dense oxide layer where almost all nanovoids were healed by the second anodizing process, which explains the low leakage current from 0 V until the dielectric breakdown (Fig. 8f). The breakdown voltage is again ~200 V below the first anodizing voltage (700 V), results that support the fundamental role of the nanovoids in the current distribution, avoiding the concentration of the current in isolated defects or voids where the dielectric breakdown can be initiated.

STEM cross-section images show in detail voids distribution through the oxide layer and the interaction of PEDOT:PSS polymer with hydrated layer and oxide layer after two cycles of voltage sweep from 0 to 400 V (Fig. 9 a, b, c) and second anodizing at 400 V (Fig. 9 d, e, f). As observed from SEM cross-section images, voids in the dielectric layer were healed, and the outer nanovoid layer generated with the post-hydration treatment remained in both conditions (Fig. 9a, 9d). The dielectric oxide layer thickness remains without any significant variation, so the primary purpose of the voltage sweep cycles and the second anodizing process is repairing the defects in the dielectric layer. The PEDOT:PSS polymer is present in

the outer nanovoid layer; the EDS area analysis reveals the presence of sulfur species (Fig. 9 c, f). The above results suggest that PEDOT:PSS does not suffer any alteration after the voltage sweep and after the second anodizing process, PEDOT:PSS can still penetrate the nanovoids layer even though this process is performed before the solid polymer capacitor is made.

It has been believed that no self-healing of physical defects occurs in the Al solid electrolytic capacitors because of the absence of a liquid electrolyte. However, the present study demonstrated clearly that physical defects in the dielectric layer of the Al solid electrolytic capacitor using PEDOT:PSS conductive polymer could be healed during the voltage sweep. A PEDOT:PSS dispersion aqueous solution containing ethylene glycol and sorbitol was used to coat a PEDOT:PSS layer. The coating should still contain ethylene glycol and sorbitol, both of which have a hygroscopic nature. Thus, it is likely that water molecules are present in the PEDOT:PSS coating, contributing to the healing of physical defects in the dielectric layer.

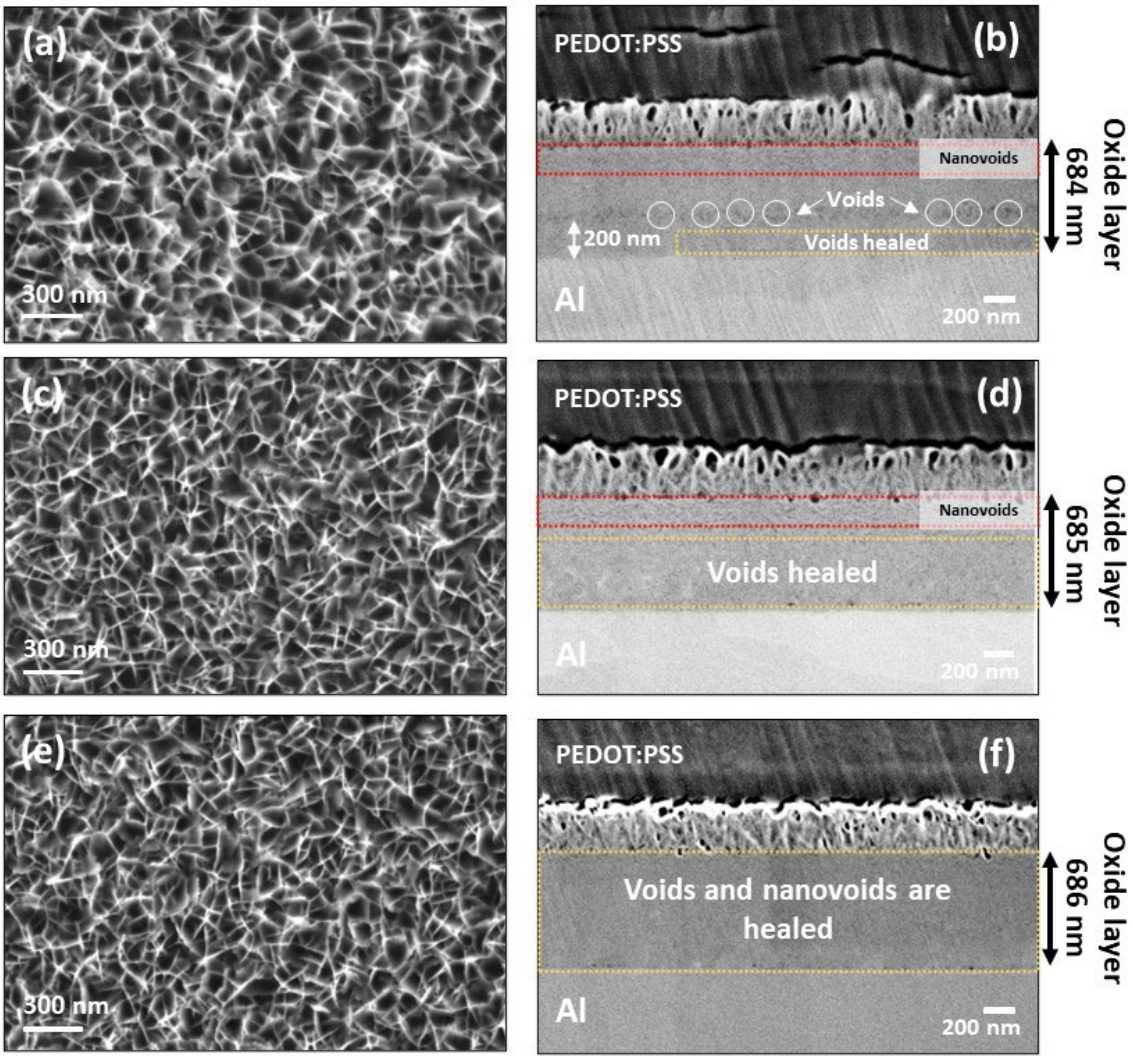

Figure 8. SEM images of the surface (a, c, and e) and cross-sections images (b, d, and f) of the anodized aluminum with post-hydration and posterior re-anodizing process at (a, b) 200 V, (c, d) 400 V and (e, f) 630 V.

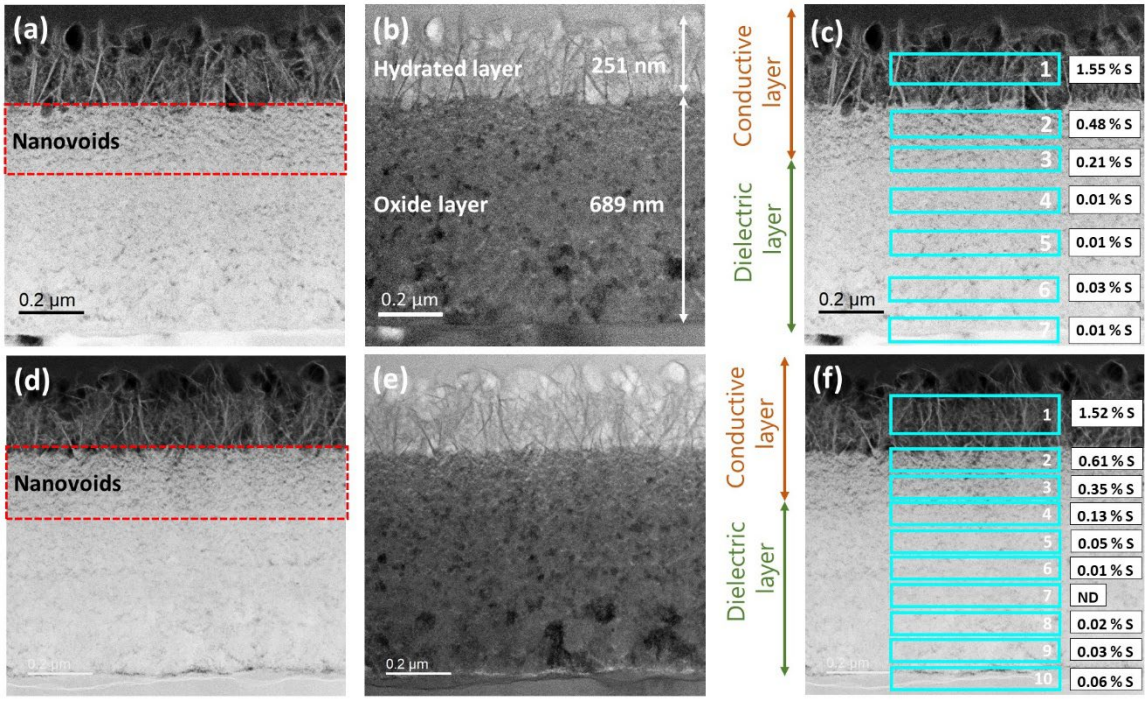

Figure 9. HAADF and (a, d) BF (b, e) scanning transmission electron micrographs of the cross-sections for the anodized aluminum with post-hydration treatment covered with PEDOT:PSS polymer after (a, b) two cycles of voltage sweep from 0 to 400 V and (d, e) and the second anodizing at 400 V. EDS area analysis, focus on % S, for the anodized aluminum with post-hydration treatment after (c) two cycles of voltage sweep from 0 to 400 V and (f) and the second anodizing at 400 V. EDS spectra and elemental composition are reported in the supporting information (Fig. S9-S10; Tables S4-S5).

The electrical properties of the capacitors after the void healing process were evaluated by AC impedance spectroscopy (Fig. 10). As described above, a deviation from the ideal dielectric behavior is observed after the post-hydration treatment due to the defects present in the oxide layer. Bode plots for the voltage sweep and the second anodization show nearly ideal capacitor behavior due to the healing of the voids. The impedance at low frequencies is

increased (highlighted by the red square), showing a more linear behavior of the impedance from low frequencies to the resonant frequency. The phase shift vs. frequency after healing of the defects in the dielectric layer also shows values close to -90° (Fig. 10a). Table 4 summarizes the capacitance, ESR, and breakdown voltage before and after the voltage sweep and second anodization. Similar capacitance values are obtained except for the second anodizing to 630 V, where the nanovoid layer is no longer present. The second anodizing to 630 V converts the nanovoid layer to a compact dielectric layer, thickening the dielectric layer and reducing the capacitance.

The complete healing of the nanovoid layer by the second anodizing at 630 V reduced the breakdown voltage significantly to ~533 V. It is important to emphasize that the presence of a nanovoids layer containing a small amount of highly dispersed PEDOT:PSS above the dielectric layer is crucial to keep the breakdown voltage above 600 V. According to the results obtained, the most promising processing route found in our study is first, dipping in hot water, second, anodizing at 700 V, then a second hot water treatment, and a second anodizing at 400 V, processing route that keeps the capacitance invariable with a breakdown voltage enhanced. On the other hand, the voltage sweep below the breakdown voltage is important due to being an in-situ process, given that it is performed with the capacitor. It is well known that applying a voltage in aluminum electrolytic capacitors allows the repair of the dielectric defects after anodizing or long-time storage conditions. Our research found similar behavior in solid conductive polymer capacitors, with an additional and straightforward treatment of immersion in hot water of the dielectric layer after anodizing as a strategy to increase the breakdown voltage.

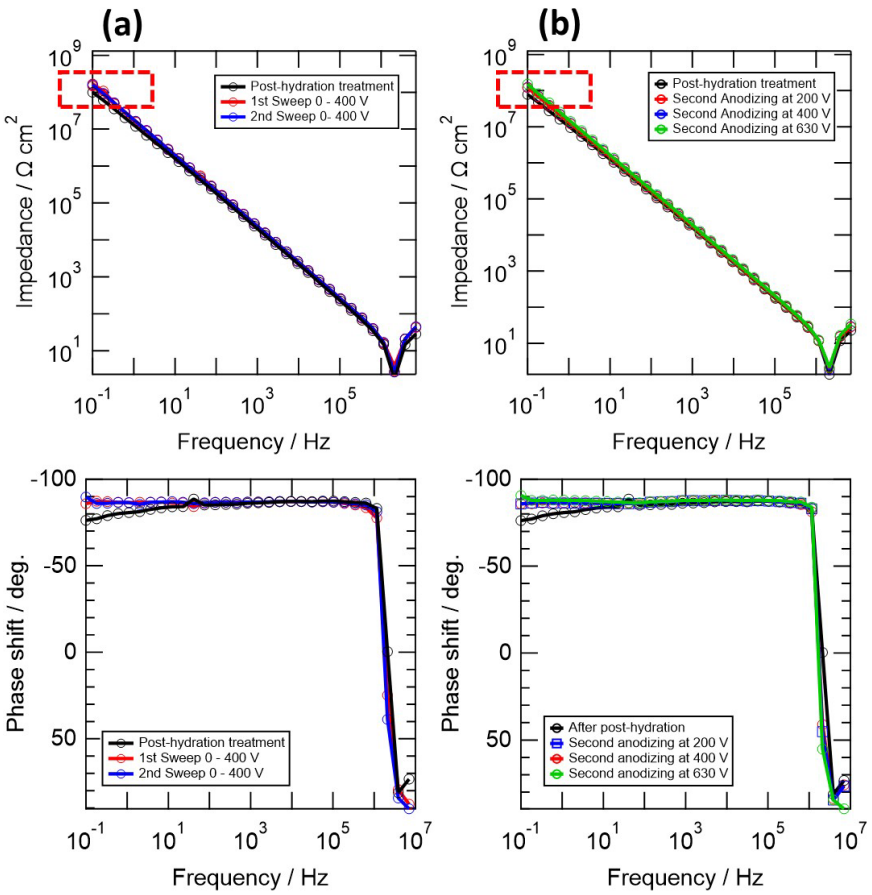

Figure 10. Bode plots of the anodized aluminum with post-hydration treatment after (a) the voltage sweep from 0 to 400 V (b) and the second anodizing.

Table 4. Capacitance and resistance of the anodized aluminum with post-hydration treatment covered with PEDOT:PSS polymer and healing process of the voids in the dielectric layer.

Condition	Capacitance, C ($nF.cm^{-2}$)	R_{ESR} ($\Omega.cm^{-2}$)	Breakdown voltage (V)
Voltage sweeping	12.34 ± 0.17	1.25 ± 0.08	818 ± 9
2nd anodizing at 200 V	12.02 ± 0.19	1.15 ± 0.06	674 ± 39
2nd anodizing at 400 V	12.06 ± 0.10	1.02 ± 0.04	669 ± 44
2nd anodizing at 630 V	10.73 ± 0.34	0.94 ± 0.02	533 ± 40

4. Conclusions

The present study demonstrates that the breakdown voltage of PEDOT:PSS-coated Al solid polymer capacitor is greatly enhanced by introducing a nanovoids-dispersed layer on the dielectric alumina layer. The nanovoids layer is formed by the post-hydration treatment after forming a dielectric alumina layer by anodizing. A small amount of PEDOT:PSS is incorporated into the nanovoids, making a nanovoids layer highly electrically resistive. This layer avoids the local current concentration at high voltages, enhancing the breakdown voltage.

The negative influence of the post-hydration treatment is the increased leakage current because the existing voids in the dielectric alumina layer are exposed to the electrolyte. However, self-healing of the physical defects in the dielectric layer occurs during voltage sweep after the PEDOT:PSS coating, reducing the leakage current. This finding provides scientific evidence of the defects healing in the dielectric layer in a solid capacitor with an electrolyte-free conductive polymer cathode. In addition, the second anodizing after the post-hydration treatment is also effective in reducing the leakage current. Even after the second anodizing, the high breakdown voltage is maintained if the nanovoids layer remains. The present study demonstrates that introducing a nanovoids-dispersed layer containing a small amount of a conductive polymer is a promising approach to developing solid capacitors with high capacitance, ripple current, thermal stability, and high withstand voltage.

Supporting information:

Experimental: Graphical illustrations of the solid polymer capacitor configuration and the experimental set-up of the AC impedance spectroscopy are observed (Figure S1-S2).

Results: the reproducibility of the experimental results (Figure S4-S5) is shown in the supporting information. Furthermore, the interaction between the PEDOT:PSS and the dielectric material is observed by the amount of S incorporated through the oxide layer due to PEDOT:PSS containing S in its chemical Formula. EDS analysis and the elemental composition (Table S1-S5) reported during the STEM analysis are shown in the supporting information (Figure S6-S10).

Acknowledgments

This study was supported in part by the MEXT-Program for Creation of Innovative Core Technology for Power Electronics. Part of this work was conducted at Hokkaido University, supported by the Nanotechnology Platform Program of the Ministry of Education, Culture, Sports, Science and Technology (MEXT), Japan Grant Numbers JPJ009777 and A-21-HK-0036.

References

(1) Slesinski, A.; Fic, K.; Frackowiak, E. New Trends in Electrochemical Capacitors. In *Advances in Inorganic Chemistry*; Elsevier, 2018; Vol. 72, pp 247–286.

(2) Su, Z.; Yao, M.; Li, M.; Gao, W.; Li, Q.; Feng, Q.; Yao, X. A Novel and Simple Aluminium/Sol–Gel-Derived Amorphous Aluminium Oxide Multilayer Film with High Energy Density. *J Mater Chem C Mater* **2018**, *6* (21), 5616–5623.

(3) Niwa, S.; Taketani, Y. Development of New Series of Aluminium Solid Capacitors with Organic Semiconductive Electrolyte (OS-CON). *J Power Sources* **1996**, *60* (2), 165–171.

(4) Primavesi, G. Aluminium Electrolytic Capacitors. In *IEE Half-Day Colloquium on Power Electronics in Traction (Digest No. 1997/324)*; IET, 1997; pp 1–4.

(5) Kudoh, Y.; Nishino, A. Recent Development in Electrolytic Capacitors and Electric Double Layer Capacitors. *Electrochemistry* **2001**, *69* (6), 397–406.

(6) Wudl, F. From Organic Metals to Superconductors: Managing Conduction Electrons in Organic Solids. *Acc Chem Res* **1984**, *17* (6), 227–232.

(7) Yamamoto, H.; Oshima, M.; Fukuda, M.; Isa, I.; Yoshino, K. Characteristics of Aluminium Solid Electrolytic Capacitors Using a Conducting Polymer. *J Power Sources* **1996**, *60* (2), 173–177.

(8) Singh, A.; Dey, A.; Das, D.; Iyer, P. K. Combined Influence of Plasmonic Metal Nanoparticles and Dual Cathode Buffer Layers for Highly Efficient RrP3HT: PCBM-Based Bulk Heterojunction Solar Cells. *J Mater Chem C Mater* **2017**, *5* (26), 6578–6587.

(9) Tu, S.; Tian, T.; Oechsle, A. L.; Yin, S.; Jiang, X.; Cao, W.; Li, N.; Scheel, M. A.; Reb, L. K.; Hou, S. Improvement of the Thermoelectric Properties of PEDOT: PSS Films via DMSO Addition and DMSO/Salt Post-Treatment Resolved from a Fundamental View. *Chemical Engineering Journal* **2022**, *429*, 132295.

(10) Moore, J. W. Nobel Prizes, 2000. *J Chem Educ* **2001**, *78* (1), 8. https://doi.org/10.1021/ed078p8.

(11) Kudoh, Y.; Akami, K.; Matsuya, Y. Solid Electrolytic Capacitor with Highly Stable Conducting Polymer as a Counter Electrode. *Synth Met* **1999**, *102* (1), 973–974. https://doi.org/https://doi.org/10.1016/S0379-6779(98)01012-1.

(12) Worfolk, B. J.; Andrews, S. C.; Park, S.; Reinspach, J.; Liu, N.; Toney, M. F.; Mannsfeld, S. C. B.; Bao, Z. Ultrahigh Electrical Conductivity in Solution-Sheared Polymeric Transparent Films. *Proceedings of the National Academy of Sciences* **2015**, *112* (46), 14138–14143.

(13) Fan, Z.; Ouyang, J. Thermoelectric Properties of PEDOT: PSS. *Adv Electron Mater* **2019**, *5* (11), 1800769.

(14) Carlberg, J. C.; Inganäs, O. Poly (3, 4-ethylenedioxythiophene) as Electrode Material in Electrochemical Capacitors. *J Electrochem Soc* **1997**, *144* (4), L61.

(15) Elschner, A.; Kirchmeyer, S.; Lovenich, W.; Merker, U.; Reuter, K. *PEDOT: Principles and Applications of an Intrinsically Conductive Polymer*; CRC press, 2010.

(16) Ju, D.; Kim, D.; Yook, H.; Han, J. W.; Cho, K. Controlling Electrostatic Interaction in PEDOT: PSS to Overcome Thermoelectric Tradeoff Relation. *Adv Funct Mater* **2019**, *29* (46), 1905590.

(17) Dekker, E.; Lasance, C. J. M. Thermal and Electrical Analysis of Solid Aluminium Capacitors. *Active and passive electronic components* **1987**, *12* (3), 167–186.

(18) Nogami, K.; Sakamoto, K.; Hayakawa, T.; Kakimoto, M. The Effects of Hyperbranched Poly (Siloxysilane) s on Conductive Polymer Aluminum Solid Electrolytic Capacitors. *J Power Sources* **2007**, *166* (2), 584–589.

(19) Nishino, A. Capacitors: Operating Principles, Current Market and Technical Trends. *J Power Sources* **1996**, *60* (2), 137–147.

(20) Conway, B. E. Capacitance Behavior of Films of Conducting, Electrochemically Reactive Polymers. *Electrochemical Supercapacitors: Scientific Fundamentals and Technological Applications* **1999**, 299–334.

(21) Ho, J.; Jow, T. R.; Boggs, S. Historical Introduction to Capacitor Technology. *IEEE Electrical Insulation Magazine* **2010**, *26* (1), 20–25.

(22) Yoo, J.; Kim, J.; Kim, Y. S. Liquid Electrolyte-Free Cylindrical Al Polymer Capacitor Review: Materials and Characteristics. *J Power Sources* **2015**, *284*, 466–480.

(23) Both, J. Electrolytic Capacitors from the Postwar Period to the Present. *IEEE Electrical Insulation Magazine* **2016**, *32* (2), 8–26.

(24) Alwitt, R. S.; Dyer, C. K.; Noble, B. Voids in Anodic Aluminum Oxide Films. *J Electrochem Soc* **1982**, *129* (4), 711.

(25) Alcalá, G.; Mato, S.; Skeldon, P.; Thompson, G. E.; Mann, A. B.; Habazaki, H.; Shimizu, K. Mechanical Properties of Barrier-Type Anodic Alumina Films Using Nanoindentation. *Surf Coat Technol* **2003**, *173* (2–3), 293–298.

(26) Xu, Y.; Thompson, G. E.; Wood, G. C. Mechanism of Anodic Film Growth on Aluminium. *Transactions of the IMF* **1985**, *63* (1), 98–103.

(27) Wood, G. C.; Skeldon, P.; Thompson, G. E.; Shimizu, K. A Model for the Incorporation of Electrolyte Species into Anodic Alumina. *J Electrochem Soc* **1996**, *143* (1), 74.

(28) Saadi, N. S.; Hassan, L. B.; Karabacak, T. Metal Oxide Nanostructures by a Simple Hot Water Treatment. *Sci Rep* **2017**, *7* (1), 7158.

(29) Hart, R. K. A Study of Boehmite Formation on Aluminium Surfaces by Electron Diffraction. *Transactions of the Faraday Society* **1954**, *50*, 269–273.

(30) Bunker, B. C.; Nelson, G. C.; Zavadil, K. R.; Barbour, J. C.; Wall, F. D.; Sullivan, J. P.; Windisch, C. F.; Engelhardt, M. H.; Baer, D. R. Hydration of Passive Oxide Films on Aluminum. *J Phys Chem B* **2002**, *106* (18), 4705–4713.

(31) Alwitt, R. S. The Anodic Oxidation of Aluminum in the Presence of a Hydrated Oxide. *J Electrochem Soc* **1967**, *114* (8), 843.

(32) Ban, C. L.; He, Y. D.; Shao, X. Effect of Trace Tartaric Acid on Anodizing of Etched Aluminum Foil for High Voltage Electrolytic Capacitor. *Journal of Materials Science: Materials in Electronics* **2013**, *24*, 3442–3447.

(33) Uchi, H.; Kanno, T.; Alwitt, R. S. Structural Features of Crystalline Anodic Alumina Films. *J Electrochem Soc* **2001**, *148* (1), B17.

(34) Ono, S. Passive Films for Electrolytic Capacitors. In *Encyclopedia of Interfacial Chemistry*; Tokio, 2018; pp 376–395.

(35) Matsuya, H.; Quintero, D.; Kitano, S.; Habazaki, H. Structure and Electric Properties of Anodized Aluminum with PEDOT:PSS Conductive Polymer Cathode. *ECS Journal of Solid State Science and Technology* **2023**, *12* (7), 073002. https://doi.org/10.1149/2162-8777/ace12b.

(36) Alwitt, R. S.; Dyer, C. K. Electrical Instability of Composite Aluminum Oxide Films. *Electrochim Acta* **1978**, *23* (4), 355–362.

(37) Pan, S.; Liang, L.; Lu, B.; Li, H. Microstructure Evolution for Oxide Film of Anodic Aluminum Foil Used in High Voltage Electrolytic Capacitor. *J Alloys Compd* **2020**, *823*, 153795.

(38) Strange, T. F.; Marshall, T. R. Very High Volt Oxide Formation of Aluminum for Electrolytic Capacitors. Patent and Trademark Office: U.S. Patent No. 6,299,752. Washington, DC: U.S October 9, 2001.

(39) Kobayashi, K.; Shimizu, K.; Teranishi, D. Crystalline Barrier Oxide Films Formed on Aluminium in an Aqueous Solution of Ammonium Dihydrogen Phosphate. *J Mater Sci Lett* **1986**, *5*, 543–544.

(40) Sato, Y.; Asoh, H.; Ono, S. Effects of Electrolyte Species and Their Combination on Film Structures and Dielectric Properties of Crystalline Anodic Alumina Films Formed by Two-Step Anodization. *Mater Trans* **2013**, *54* (10), 1993–1999.

(41) Gnonhoue, O. G.; Velazquez-Salazar, A.; David, É.; Preda, I. Review of Technologies and Materials Used in High-Voltage Film Capacitors. *Polymers (Basel)* **2021**, *13* (5), 766.

(42) Torki, J.; Joubert, C.; Sari, A. Electrolytic Capacitor: Properties and Operation. *J Energy Storage* **2023**, *58*, 106–330.

(43) Lim, K. J.; Park, S. G.; Kang, S. H.; Kim, S. H.; Han, M. H. Dielectric Properties of Aluminium Solid Electrolytic Capacitor Using Conduction Polymer. In *Proceedings of 1994 4th International Conference on Properties and Applications of Dielectric Materials (ICPADM)*; IEEE, 1994; Vol. 1, pp 223–226.

(44) Ban, C.-L.; Wang, F.-R.; Chen, J.-H.; Liu, Z.-Q. Effect of Hydration on Microstructure and Property of Anodized Oxide Film for Aluminum Electrolytic Capacitor. *Journal of Materials Science: Materials in Electronics* **2018**, *29*, 16166–16171.

(45) Takahashi, H.; Yamagami, M.; Furuichi, R.; Nagayama, M. FTIR Analysis of Hydroxide Films on Aluminum. *Hyomen Kagaku* **1987**, *8* (4), 279–281.

(46) Alwitt, R. S. The Growth of Hydrous Oxide Films on Aluminum. *J Electrochem Soc* **1974**, *121* (10), 1322.

(47) Verwey, E. J. W. The Structure of the Electrolytical Oxide Layer on Aluminium. *Zeitschrift für Kristallographie-Crystalline Materials* **1935**, *91* (1–6), 317–320.

(48) Takahashi, H.; Yamaki, M.; Furuichi, R. The Role of Anions in the Formation of Hydroxide Films on Aluminum in Hot Aqueous Solutions. *Corros Sci* **1990**, *31*, 243–248.

(49) Takahashi, H.; Sakairi, M.; Kikuchi, T. Anodic Oxide Films on Aluminum: Their Significance for Corrosion Protection and Micro-and Nano-Technologies. In *Progress in Corrosion Science and Engineering I: Progress in Corrosion Science and Engineering I*; Springer, 2009; pp 59–174.

(50) Chi, C.-S.; Jeong, Y.; Ahn, H.-J.; Lee, J.-H.; Kim, J.-G.; Lee, J.-H.; Jang, K.-W.; Oh, H.-J. Transition of Hydrated Oxide Layer for Aluminum Electrolytic Capacitors. *Materials Science and Engineering: A* **2007**, *449*, 314–317.

(51) Takano, T.; Matsuya, H.; Kowalski, D.; Kitano, S.; Aoki, Y.; Habazaki, H. Raman and Glow Discharge Optical Emission Spectroscopy Studies on Structure and Anion Incorporation Properties of a Hydrated Alumina Film on Aluminum. *Appl Surf Sci* **2022**, *592*, 153321.

(52) Takahashi, H.; Umehara, Y.; Furuichi, R.; Nagayama, M. Anodizing of Aluminum Covered with Hydroxide III Effect of Anodizing Temperature on the Void Distribution in the Composite Oxide Film. *Journal of The Surface Finishing Society of Japan* **1989**, *40* (4), 590–597.

(53) Takahashi, H.; Nagayama, M. Electrochemical Behaviour and Structure of Anodic Oxide Films Formed on Aluminium in a Neutral Borate Solution. *Electrochim Acta* **1978**, *23* (3), 279–286.

(54) Abdennadher, K.; Venet, P.; Rojat, G.; Rétif, J.-M.; Rosset, C. A Real-Time Predictive-Maintenance System of Aluminum Electrolytic Capacitors Used in Uninterrupted Power Supplies. *IEEE Trans Ind Appl* **2010**, *46* (4), 1644–1652.

(55) Evangelisti, F.; Stiefel, M.; Guseva, O.; Nia, R. P.; Hauert, R.; Hack, E.; Jeurgens, L. P. H.; Ambrosio, F.; Pasquarello, A.; Schmutz, P. Electronic and Structural Characterization of Barrier-Type Amorphous Aluminium Oxide. *Electrochim Acta* **2017**, *224*, 503–516.

(56) Yim, K.; Yong, Y.; Lee, J.; Lee, K.; Nahm, H.-H.; Yoo, J.; Lee, C.; Seong Hwang, C.; Han, S. Novel High-κ Dielectrics for next-Generation Electronic Devices Screened by Automated Ab Initio Calculations. *NPG Asia Mater* **2015**, *7* (6), e190–e190.

(57) Clark, R. D. Emerging Applications for High K Materials in VLSI Technology. *Materials* **2014**, *7* (4), 2913–2944.

(58) Ban, C.-L.; He, Y.-D.; Xin, S. Effect of Citric Acid on Microstructure and Electrochemical Characteristics of High Voltage Anodized Alumina Film Formed on Etched Al Foils. *Transactions of Nonferrous Metals Society of China* **2011**, *21* (1), 133–138.

(59) Pan, S.; Liang, L.; Lu, B.; Li, H.; Li, Y. Effect of Azelaic Acid on Microstructure Evolution and Electrical Properties of Anodic Aluminum Foil for Electrolytic Capacitor. *Journal of Materials Science: Materials in Electronics* **2021**, *32* (2), 2579–2589.

(60) Hung, C. Y.; Lung, O. Bin; Lien, L. Y. Effect of Acid Concentration and Current Density on DC Etching of Aluminum Electrolytic Capacitor Foil. *Korean Journal of Chemical Engineering* **2007**, *24*, 881–887.

(61) Ban, C.; He, Y.; Shao, X.; Wang, L. Anodizing of Etched Aluminum Foil Coated with Modified Hydrous Oxide Film for Aluminum Electrolytic Capacitor. *Journal of Materials Science: Materials in Electronics* **2014**, *25*, 128–133.

(62) Yoshimura, S.; Itoh, Y.; Yasuda, M.; Murakami, M.; Takahashi, S.; Hasegawa, K. An Aluminum Solid Electrolytic Capacitor with an Organic Semiconductor Electrolyte. *IEEE Transactions on Parts, Hybrids, and Packaging* **1975**, *11* (4), 315–321.

(63) Yamamoto, H.; Oshima, M.; Hosaka, T.; Isa, I. Solid Electrolytic Capacitors Using an Aluminum Alloy Electrode and Conducting Polymers. *Synth Met* **1999**, *104* (1), 33–38.

(64) Zhang, Y.; Feng, H.; Wu, X.; Wang, L.; Zhang, A.; Xia, T.; Dong, H.; Li, X.; Zhang, L. Progress of Electrochemical Capacitor Electrode Materials: A Review. *Int J Hydrogen Energy* **2009**, *34* (11), 4889–4899.

(65) Buhrkal-Donau, S.; Ebel, T. 5.4. A Way to High Voltage Polymer Aluminium Electrolytic Capacitors. **2021**.

(66) Okudaira, K.; Asoh, H.; Ono, S. Effect of Electrolyte Species on Dielectric Property of Crystalline Anodic Alumina Film. *Electrochemistry* **2007**, *75* (11), 873–878.

(67) Hasegawa, H.; Suganuma, E.; Funakoshi, A. Formation and Structure of Hydrated/Composite Oxide Films on Aluminum. *Journal of The Surface Finishing Society of Japan* **1989**, *40* (12), 1422–1426.

1 **Abstract graphic**

2

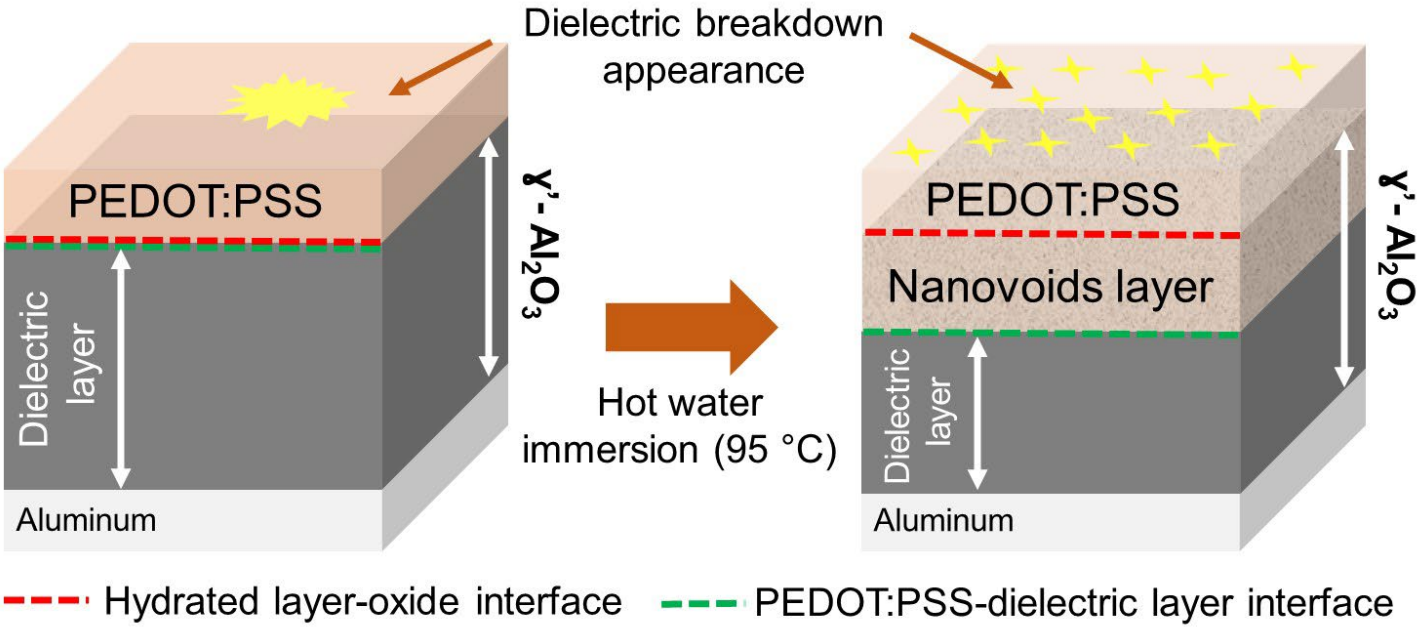

4